AN EFFECT OF A WEAK COMPRESSIBILITY ON TUBULAR VORTICES IN DECAYING ISOTROPIC TURBULENCE

Hideaki Miura
Theory and Computer Simulation Center,
National Institute for Fusion Science,
Oroshi 322-6, Toki, Gifu 509-5292, Japan
miura@toki.theory.nifs.ac.jp

ABSTRACT

We investigate effects of a weak compressibility on turbulence by means of vortex identification. A vortex identification scheme developed by Miura and Kida (1997), and Kida and Miura(1998a) for an incompressible fluid is extended to compressible fluids, to analyze statistical nature of vortices in compressible turbulence. It is shown through this analysis that a weak compressibility makes total volume of vortex cores of compressible turbulence smaller than that of incompressible turbulence. Radius of vortices in compressible turbulence tends to be smaller and less uniform than their incompressible counter parts. Relations between our vortex analysis and previous investigations for compressible homogeneous turbulence and mixing layers are discussed.

INTRODUCTION

Vortex dynamics is one of the key issues to understand physics of turbulence, whether a fluid is compressible or incompressible. On one hand, vortical structures and their dynamics in turbulence have been investigated extensively on incompressible fluids. One of a main difficulty on vortex investigation is that there is not sufficient consensus on an *objective* definition of a vortex. In order to identify vortical structures in turbulence, several schemes or criteria have been proposed. See a review by Kida and Miura (1998b) and references therein on this problem.

On the other hand, one of a main issues of a compressible turbulence in the last decade has been to clarify compressibility effects on turbulence. Especially, a mechanism to suppress growth rate of the kinetic energy in mixing layers or other sheared turbulence has been extensively investigated. Sarkar(1995) has shown for homogeneous shear turbulence that one of the most important contributions of the compressibility came from modification of rotational components of the velocity rather than from dilatational terms. Vreman et al.(1996) have also denied importance of dilatational terms and shown importance of the pressure-strain term in the evolution equation of the Reynolds stress for a compressible mixing layer. Both of them emphasized an importance of contributions of rotational components of the velocity to the suppression of the growth rate of the kinetic energy through Reynolds stress tensor.

While compressibility effects have been investigate from a point of view of the kinetic energy growth, detailed physical mechanism on the point how the compressibility changes the rotational component of the velocity remains unclarified. In this article, we aim to investigate this problem from a point of view of vortex dynamics. Comprehending how vortex structures and their dynamics in turbulence are modified by the compressibility should contribute to understand compressible turbulence. We focus on tubular vortices in an isotropic compressible turbulence and study effects of a weak compressibility on vortices by means of numerical simulations and a vortex identification scheme.

NUMERICAL SIMULATIONS

Basic equations and initial conditions

Motions of an incompressible fluid with the unit density is described by the continuity equation

$$\frac{\partial u_i}{\partial x_i} = 0 \qquad (1)$$

and the Navier-Stokes equation

$$\frac{\partial u_i}{\partial t} = -u_j \frac{\partial u_i}{\partial x_j} - \frac{\partial p}{\partial x_i} + \frac{1}{Re_0} \frac{\partial^2 u_i}{\partial x_j \partial x_j} \quad (i = 1, 2, 3) \qquad (2)$$

We take a sum from 1 to 3 over repeated suf-

fices. Motions of a compressible fluid is described by a set of equations

$$\frac{\partial \rho}{\partial t} = -\frac{\partial (\rho u_i)}{\partial x_i} \quad (3)$$

$$\frac{\partial (\rho u_i)}{\partial t} = -\frac{\partial (\rho u_i u_j)}{\partial x_j} - \frac{\partial p}{\partial x_i} + \frac{2}{Re_0}\frac{\partial}{\partial x_j}\left\{S_{ij} - \frac{1}{3}\delta_{ij}\left(\frac{\partial u_k}{\partial x_k}\right)\right\} \quad (i = 1, 2, 3) \quad (4)$$

$$\frac{\partial E_T}{\partial t} = -\frac{\partial}{\partial x_i}\left[(E_T + p)u_i\right] + \frac{1}{{M_0}^2 Pr_0 Re_0(\gamma - 1)}\frac{\partial^2 T}{\partial x_i \partial x_i} + \frac{2}{Re_0}\frac{\partial}{\partial x_j}\left\{u_i\left[S_{ij} - \frac{1}{3}\delta_{ij}\left(\frac{\partial u_k}{\partial x_k}\right)\right]\right\} \quad (5)$$

$$E_T = \frac{p}{\gamma - 1} + \frac{1}{2}\rho u_i u_i \quad (6)$$

$$p = \frac{1}{\gamma M_0^2}\rho T \quad (7)$$

where ρ, p, T and E_T represents the density, pressure, temperature and total energy, respectively. The symbol u_i represents the i-th component of the velocity vector and S_{ij} represents (i, j) component of the rate-of-strain tensor $S_{ij} = \frac{1}{2}(\partial u_i/\partial x_j + \partial u_j/\partial x_i)$. Control parameters Re_0, Pr_0 and M_0 are the Reynolds number, Prandtl number and Mach number, respectively.

In order to compare behaviors of the fluid governed by these two sets of equations, we adopt two conditions as follows:

1. The same Reynolds number Re_0 is adopted for both compressible and incompressible Navier-Stokes equations.
2. The rotational components of the velocity are the same in these two sets of equations at the initial time.

Then behaviors of these two sets of equations should be similar each other at an initial stage of simulations. Deviations of compressible solution from incompressible one is considered to come from either explicit or implicit compressible effects. Furthermore, if we adopt an uniform initial density $\rho = 1$ and initial pressure fluctuation obtained by solving the Poisson equation

$$\frac{\partial^2 \tilde{p}}{\partial x_j \partial x_j} = -\frac{\partial^2 \left(u_i^I u_j^I\right)}{\partial x_i \partial x_j} \quad (8)$$

	N^3	Re_0	M_0^2	Pr_0	γ
I-1	256^3	500	-	-	-
C-1	256^3	500	2.0	0.70	1.4
I-2	256^3	1000	-	-	-
C-2	256^3	1000	2.0	0.70	1.4

Table 1: Resolution and parameters of compressible and incompressible simulations.

effects of variable density for compressible simulations become quite small. The quantity $\tilde{p}$ is often called "incompressible pressure". (See Elrebacher et al.(1990), for example.) In eq.(8), the superscript I represents the rotational components of the velocity.

In order to make this comparison, we execute four simulations of decaying isotropic turbulence whose initial conditions are described as follows.

1. The rotational components of the velocity field are given by a fixed energy spectrum $E(k) \propto (k/k_0)^4 exp\left[-2(k/k_0)^2\right]$ $(k_0 = 4)$ and randomized phases. Compressible components of the velocity is null first.
2. The initial density of compressible simulations is unity.
3. The initial pressure fluctuation of compressible simulations is given by eq.(8).

Control parameters and resolution of the simulations are shown in Table 1. The symbols C and I represents compressible and incompressible runs, respectively.

In all of our simulations, triply-periodic boundary condition on a $2\pi \times 2\pi \times 2\pi$ cube are imposed. We adopt the pseudo-spectral method and the Runge-Kutta-Gill scheme to solve the two systems (1)-(2) and (3)-(7). The aliasing errors are removed by the truncation procedure.

Vortex identification

Before looking closely into numerical results, we quickly review how to identify tubular vortices in turbulence, and describe how to apply the scheme to compressible turbulence. The scheme we exploit here is described in Miura and Kida (1997), and Kida and Miura (1998a, 1998b) for incompressible turbulence.

First, we assume that a fluid is incompressible. The inertia which works to a fluid can be written as

$$u_j \frac{\partial u_i}{\partial u_j} = -\frac{\partial P}{\partial x_i} + \epsilon_{ijk}\frac{\partial Q_k}{\partial x_j} \quad (9)$$

where the first and the second terms in the right-hand side of this equation represent potential components and torque of the inertia.

The quantity P coincides with the pressure if a fluid is incompressible and the periodic boundary condition is imposed to the all directions. Note that the potential P never coincides with the pressure when a fluid is compressible, or a boundary condition is not appropriate even when it is a incompressible fluid.

We make use of a fact that a two-dimensional well of the potential P is tends to be formed in order to balance with the centrifugal force of a swirling motion of a vortex. We represent the eigenvalues of the Hessian of the potential P by $\lambda^{(i)}$ $(i = 1, 2, 3)$,

$$\lambda^{(1)} \geq \lambda^{(2)} \geq \lambda^{(3)} \qquad (10)$$

If two eigenvalues are positive, the potential P has a two-dimensional local minimum on the plane perpendicular to the normal vector $\mathbf{e}^{(3)}$, which is the eigenvector associated with the eigenvalue $\lambda^{(3)}$.

By calculating eigenvalues of the Hessian of P over all of the grid points of a simulation box, we obtain a set of candidate points to construct central axes of vortices. However, existence of sectional minimum of P does not necessarily imply existence of swirling motions on these candidate points. In order to remove points without swirling motions, we impose a swirl condition as follows. Suppose that (X_1, X_2) is a local, two-dimensional Cartesian coordinate whose directions are determined by two eigenvectors $\mathbf{e}^{(1)}$ and $\mathbf{e}^{(2)}$. A candidate of vortex axes is located at the center of this coordinate system. We project three-dimensional velocity relative to the origin of this coordinate system on this plane and linearize it as

$$\begin{bmatrix} V_1 \\ V_2 \end{bmatrix} = \begin{bmatrix} W_{11} & W_{12} \\ W_{21} & W_{22} \end{bmatrix} \begin{bmatrix} X_1 \\ X_2 \end{bmatrix} = \overline{\mathbf{A}} \begin{bmatrix} X_1 \\ X_2 \end{bmatrix} \qquad (11)$$

where V_i is the i-th component of the projected velocity field and W_{ij} is the (i, j) component of the rate-of-strain tensor on this coordinate system. When the matrix $\overline{\mathbf{A}}$ has the complex eigenvalues, streamlines of the projected velocity field are spiral. It is simply represented by the negative value of the discriminant D of the eigen-equation:

$$D = (W_{11} - W_{22})^2 + 4W_{12}W_{21} \leq 0 \qquad (12)$$

We impose this condition to all of the candidates of vortex axes and discards them if the swirl condition is not satisfied. At last, we connect the candidates which have survived the examination by the swirling condition, to construct swirling axes of vortices. Vortex cores are defined here as regions where the swirling condition $D \leq 0$ is satisfied around vortex axes.

Swirling axes of vortices in compressible turbulence can be constructed by the process described above. However, we modify the scheme here. In stead of using the velocity in compressible turbulence, we make the Helmholtz decomposition of the velocity and adopt the rotational component. As far as the compressibility is quite weak, the original scheme and modified one give almost the same results. However, they give different results when the compressibility becomes stronger. We should be careful to choose which approach to be adopted in view of what we aim to analyze. Now we adopt the latter approach because we are going to investigate change of the rotational components of velocity by a compressibility effects.

WEAKLY COMPRESSIBLE TURBULENCE

Here we compare numerical results obtained by the simulations C-1, C-2, I-1 and I-2.

Time evolution of the kinetic energy per unit density $\left\langle \frac{1}{2} u_i u_i \right\rangle$ are shown in Fig.1. Here the bracket $\langle\ \rangle$ represents the volume average. Black diamonds and black boxes represent the kinetic energy of C-1 and C-2, respectively, while the kinetic energies of I-1 and I-2 are represented by dotted and solid lines, respectively. As far as we do not write explicitly, the symbols and lines are used in the same manner with Fig.1 in figures shown later.

Since the compressibility is quite weak in the runs C-1 and C-2, their kinetic energies are almost the same with I-1 and I-2, respectively. Recall that one of a central topic of a compressible turbulence has been to clarify the reduction mechanism of the growth rate of the kinetic energy. Although the kinetic energy of a compressible isotropic turbulence tends to be smaller than its incompressible counter part when the compressibility is stronger, it is not the case.

Time evolution of the enstrophy is shown in Fig.2. The enstrophy of C-1 is almost the same with that of I-1. However, The enstrophy of C-2 grows and decays faster than that of I-2. It means that small scale structures are more energetic in C-2 than in I-2 simulation.

In Fig.3(a) and (b), vortex axes identified in simulations C-2 and I-2 identified are shown, respectively, at $t \simeq 3$. It is a time when enstrophy of these two runs are going to take

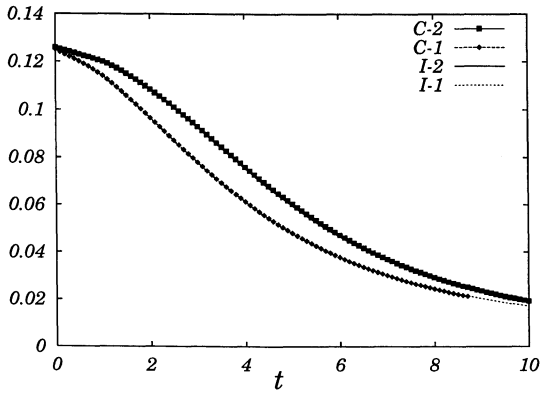

Figure 1: Time evolution of the kinetic energy per unit mass. Black diamonds and black boxes represent the kinetic energy of C-1 and C-2, respectively. The kinetic energies of I-1 and I-2 are represented by dotted and solid lines, respectively.

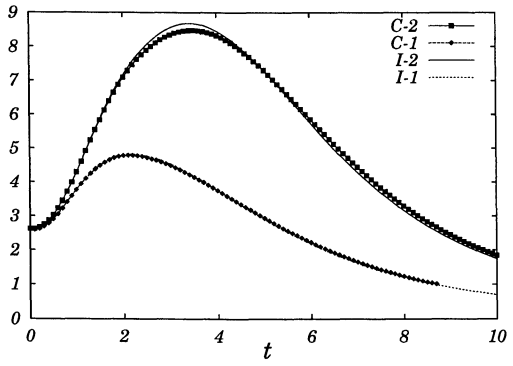

Figure 2: Time evolution of the enstrophy.

their maximum values and new axes are actively generated. The size of regions shown in Figs.3 are $128 \times 128 \times 128$ grid points out of entire $256 \times 256 \times 256$ grid points. When we observe relatively long vortex axes in Fig.3(a), we are able to find its counter part in Fig.3(b) and vice versa. However, there are many pieces of vortex axes in Fig.3(a) which are relatively short and we are often fail to find their counter parts in Fig.3(b).

In Fig.4, total length of vortex axes are shown. Difference of the length between C-1 and I-1, C-2 and I-2 respectively, are very small. While there are much more number of vortex axes observed in Fig.3(a) than in Fig.3(b), total length of vortex axes in these two simulations are comparable. One possible scenario to achieve this is that some of compressible vortex axes are torn off (presumably by a compressibility effect) in the course of their time evolution and advected to other places. Although we need to track several vortices in time direction in order to verify this scenario, it goes over a scope of this article.

Total volume of vortex cores are shown in Fig.5. It is seen that total volume of vortex

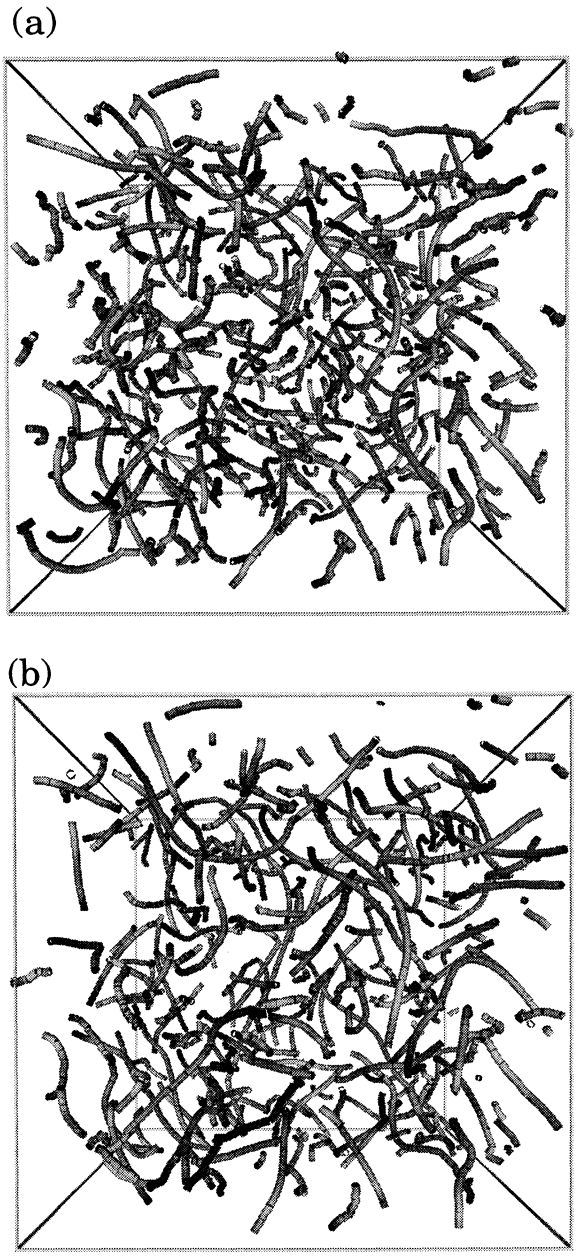

Figure 3: Vortex axes identified for (a)run C-2 and (b)I-2. Number of grid points of these figures are $128 \times 128 \times 128$ out of $256 \times 256 \times 256$ entire system.

cores in compressible turbulence tends to be smaller than incompressible ones. Since the total length of vortex axes are almost the same between C-2 and I-2, it suggests that the vortex axes in C-2 are much more slender than those in I-2.

In order to compare thickness of vortices in compressible and incompressible turbulence, we make use of the virtual radius R which was defined by Kida and Miura(1998a). It is the mean distance of the outermost enclosure of a vortex core from the center of gravity of the vortex cross section associated with the vortex core. The probability density functions

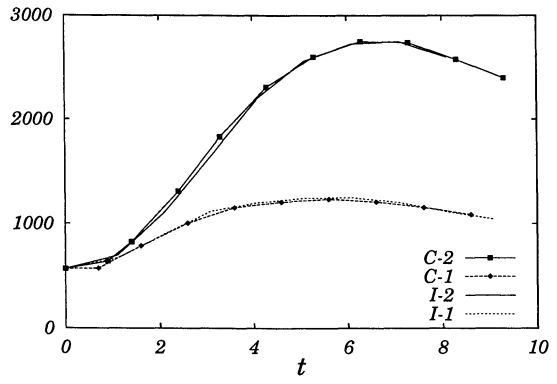

Figure 4: Total length of central axis of vortices.

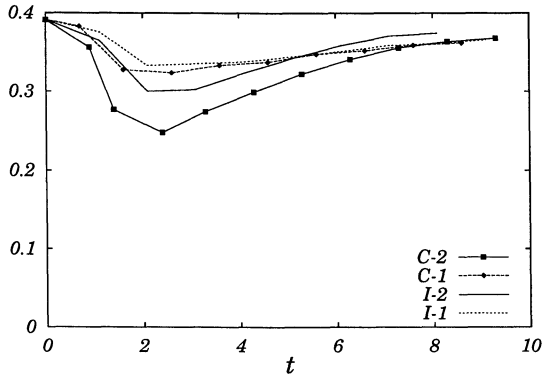

Figure 5: Ratio of volume occupied by vortex cores to the entire region.

(pdfs) of the virtual radius R of vortices for the runs C-2 and I-2 are shown in Fig.6. It is clearly seen that vortex cores tends to have larger R in I-2 than in C-2. Since the Kolmogorov's length scale l_K is about 0.015 at this time for I-2, the peak of these pdfs are located at $R \simeq 6.5\ l_K$. However, the peak the pdf shifts toward smaller R in a course of time evolution, to be locate at around $R \simeq 4\ l_K$, which is consistent with the pdf shown in Kida and Miura(1998a).

Typical vortex cores in runs C-2 and I-2 are shown in Fig.7(a) and (b), respectively. Thickness of vortex cores in Fig.7(a) vary from lower side to upper side, having non-uniform structures. On the other hand, vortex cores in Fig.7(b) look slender, having almost uniform thickness. The upper parts of vortex cores in Fig.7(a) is quite thinner than those in Fig.7(b), while lower part are quite thicker. Thus, we are not able to assert simply that vortex cores in compressible turbulence is thinner or thicker than those in incompressible turbulence. Our observation shows that a characteristic of compressible vortices is a non-uniformity of vortex thickness. Furthermore, the top part of vortex cores in Fig.7(a) is completely separated from the main body of these vortex cores. It supports the deduction that the vortex axes are torn off and advected away, without changing total length of vortex axes.

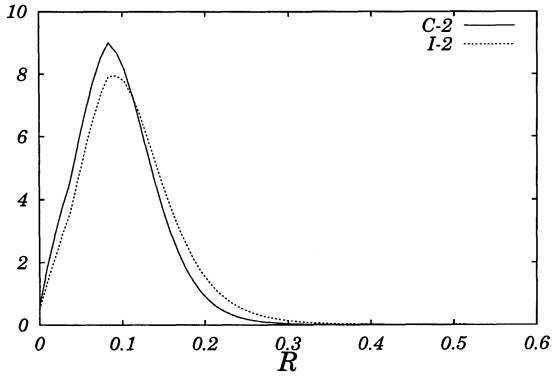

Figure 6: Probability distribution functions of the virtual radius R of vortex cores in C-2 (solid lines) and I-2 (dashed lines).

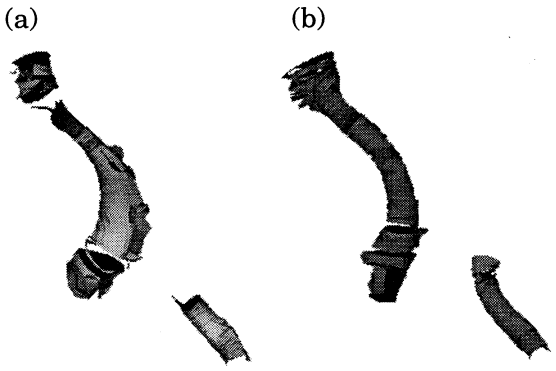

Figure 7: Typical vortex cores obtained by runs (a)C-2 and (b)I-2.

CONCLUDING REMARKS

We have conducted simulations of compressible and incompressible isotropic turbulence with the same initial velocity field and the same Reynolds number. In our compressible simulations, the kinetic energy per unit density was almost the same between compressible and incompressible turbulence. There was no obvious compressibility effect such as a suppression of growth rate of the kinetic energy, which is often observed in homogeneous shear flows and mixing layers. A small difference between compressible and incompressible simulation was observed in the time evolution of enstrophy. These facts implies that compressibility effects are quite weak in our simulations, to be observed only in small scale structures.

We have identified vortex axes and cores in compressible and incompressible turbulence, to

compare their statistical natures. It was observed that compressible vortices have smaller total volume, smaller mean radius of than incompressible vortices though total length of vortex axes are almost the same between compressible and incompressible simulations. Furthermore, thickness of vortex structures in compressible turbulence were less uniform than those in incompressible turbulence. We would like to emphasize that vortex structures are strongly coupled with behaviors of Reynolds stress tensor, by definition. In this articles, we investigated vortex structures by using the rotational components of the velocity. Thus these vortex structures are good representatives of compressibility effects which were investigated by Sarkar(1995) and Vreman et al.(1996). It should be noteworthy that clear differences were observed between vortex structures in compressible and incompressible turbulence even when the compressibility was so weak. We deduce that a modification of vortex structures by the compressibility contributes to suppression of the kinetic energy observed in homogeneous shear turbulence or mixing layers. In order to clarify this modification mechanism, we should track time evolution of single vortex structure and various physical quantities such as strain-rate-tensor, dilatation and so on which are considered to affect it. Results of analysis of time evolution should be reported in our next article.

This simulation research was conducted by making use of the supercomputer NEC SX-4/64M2 in the Theory and Computer Simulation Center of National Institute for Fusion Science. This work was partially supported by a Grant-in-Aid for Scientific Research from the Ministry of Education, Culture, Science and Technology in Japan.

References

Erlebacher, G. et al., 1990, "The Analysis and Simulation of Compressible Turbulence", *Theoret. Comput. Fluid Dynamics*, Vol. 2, pp. 73-95.

Kida, S. and Miura, H., 1998a, "Swirl Condition on a Low-Pressure Vortices", *J. Phys. Soc. Japan*, Vol. 67, pp. 2166-2169.

Kida, S. and Miura, H., 1998b, "Identification and Analysis of Vortical Structures", *Euro. J. Mech. B/Fluids*, Vol. 17, pp. 471-488.

Miura, H. and Kida, S., 1994, "Vorticity Generation by Shock-Vorticity Interaction", *J. Phys. Soc. Japan*, Vol. 63, pp. 4000-4010.

Miura, H. and Kida, S., 1997, "Identification of Tubular Vortices in Turbulence", *J. Phys. Soc. Japan*, Vol. 66, pp. 1331-1334.

Sarkar, S. 1995, "The stabilizing effect of compressibility in turbulent shear flow", *J. Fluid Mech.*, Vol. 282, pp. 163-186.

Vreman, A. W. et al, 1996, "Compressible mixing layer growth rate and turbulence statistics", *J. Fluid Mech.*, Vol. 320, pp. 235-258.